Wear 268 (2010) 1285–1294

Contents lists available at ScienceDirect

Wear

journal homepage: www.elsevier.com/locate/wear

Asperity creep under constant force boundary conditions

Andreas Goedecke[a,b,*], Robert L. Jackson[c], Randolf Mock[b]

[a] Institute of Technical Mechanics, Johannes Kepler University, Altenbergerstrasse 69, 4040 Linz, Austria
[b] Actuator and Drive Systems, Siemens Corporate Technology, Otto-Hahn-Ring 6, 81379 Munich, Germany
[c] Department of Mechanical Engineering, Auburn University, Auburn, AL 36830, USA

ARTICLE INFO

Article history:
Received 18 July 2009
Received in revised form 24 January 2010
Accepted 27 January 2010
Available online 4 February 2010

Keywords:
Asperity
Creep
Spherical contact
Garofalo creep law

ABSTRACT

This work presents an analysis of the transient creep deformation of a hemisphere in contact with a rigid flat, loaded by a constant force. The analysis is based on extensive finite element simulations, using a Garofalo creep law. Motivated by the simulations, an analytical framework is derived. Starting from the trivial case of a cylinder, the analytical framework can be generalized by exchanging a few functionals; this will describe the spherical geometry under analysis. The necessary functionals are derived by using a combination of analytical and empirical models. The resulting model accurately predicts the creep evolution of arbitrary asperities for a wide parameter range, requiring only the bulk material parameters. The results are interpreted in view of transient friction effects with creep as their possible cause.

1. Introduction

The contact of an elastic-perfectly plastic hemisphere with a rigid flat has been studied intensively in recent times (see [1–7]). These models are usually studied from the perspective of the contact and friction between rough surfaces. Here, the hemisphere serves as a model for a contacting surface asperity or micro-junction. Especially important in this context is the derivation of universal laws for the asperity behavior, to be embedded in statistical (e.g. the seminal Greenwood–Williamson model [8]) or fractal or multiscale models (e.g., [9]) of surface contact.

The classic Hertz [10] theory of hemisphere contact has been extended by studies of the elasto-plastic transition region [1,2,4], while recent research efforts have included a combination of normal and tangential loading [11,12], loading and unloading [3,13,14,7], adhesion [15,5], or electromagnetic effects [16], among others. The analysis of creep deformation of asperities has received increasing attention (see [6,17,18]).

On the other hand, recent experimental research [19,20] has supported the early conjectures by Moore and Tabor [21], Spurr [22], Rabinowicz [23] and others that the emergence of transient friction laws are linked to asperity deformation through creep. Theoretical analyses have supported this theory (e.g., [24,25]). Among the effects describable by this creep theory are the dwell-time dependent rise in static friction [21,22], the velocity-dependent dynamic friction [26] or friction lag and hysteresis [27]. This highlights the importance of analyzing the creep deformation of asperities.

In Goedecke and Mock [18], the creep of an asperity under a constant displacement or interference boundary condition was analyzed. In the present paper, the analysis is extended to the transient creep behavior of an asperity under a constant *force* boundary condition. The empirical laws presented in Goedecke and Mock [18] are extended to present a comprehensive one-dimensional model for this situation. This study aims both at developing a quantitative understanding of the creep deformation of an asperity and finding a quantitative model embeddable in a contact model for rough surfaces.

2. Modeling and simulation

The geometry under analysis is a half-sphere with an undeformed radius R in contact with a rigid flat as shown in Fig. 1a. Due to the symmetry, only a quarter sphere has to be considered, using an axial symmetric element formulation. At the base of the sphere, a sliding boundary condition has been implemented, in line with Kucharski et al. [28] and Kogut and Etsion [1].

The commercial finite element simulation code ANSYS 11 was used to perform the simulations. A mesh of about 3300 predominantly rectangular elements with quadratic shape functions was

* Corresponding author at: Actuators and Control, Siemens Corporate Technology, 81379 Munich, Germany. Tel.: +49 1781874476; fax: +49 8963646881.
E-mail addresses: Andreas.Goedecke@students.jku.at (A. Goedecke), robert.jackson@eng.auburn.edu (R.L. Jackson), Randolf.Mock@siemens.com (R. Mock).

0043-1648/$ – see front matter © 2010 Elsevier B.V. All rights reserved.
doi:10.1016/j.wear.2010.01.025

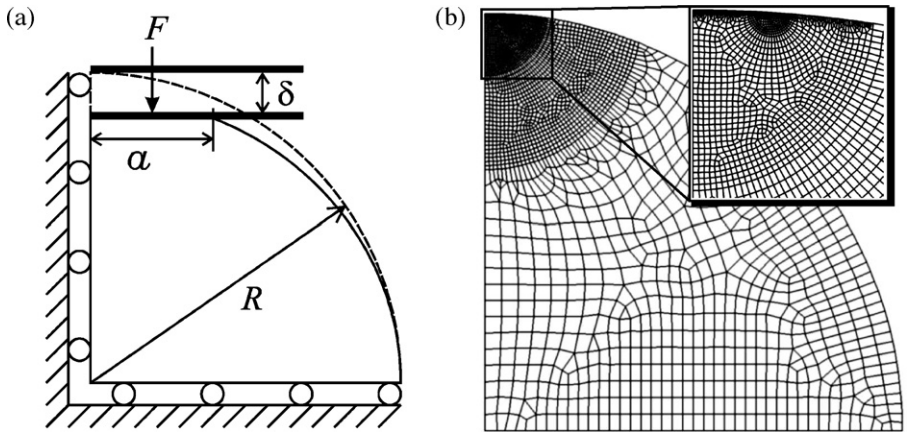

Fig. 1. (a) Sketch of the geometry. (b) The finite element mesh used for the simulation.

constructed, with meshing based on a series of regions. A fine mesh was used in proximity to the contact area, with increasingly coarser meshes towards the region near the base of the sphere [18]. See Fig. 1b for a graphical representation of the mesh. The following mesh parameters were typically used: a semicircular region with a radius of $0.15R$ centered on the uppermost tip of the sphere was meshed with a default mesh size of approximately $0.005R$. In a semicircular region centered on the outer rim of the contact zone with a radius of $0.02R$, the default mesh size was reduced to $0.002R$. In a wider region of semicircular shape with a radius of $0.38R$ around the sphere tip, the mesh size was increased to $0.01R$ with no refinement near the boundary. This meshing region was sized to comprise the high-stress regions of the model. The rest of the model was meshed with a mesh size of $0.04R$.

For the contact, a rigid line target element was chosen to model the rigid flat and a purely Lagrangian contact algorithm to implement the contact condition. The contact radius a (see Fig. 1a), contact force F, and interference δ were measured every time a node established or lost contact with the rigid flat. ANSYS' geometrically nonlinear formulation (ANSYS keyword NLGEOM) was activated, corresponding to a Lagrangian strain formulation. An isotropic and elastic-perfectly plastic material model was chosen while no hardening rule was used. The plasticity behavior was based on the (isotropic) von Mises yielding criterion, with an associative flow rule.

Standard continuum theory (e.g., [29]) states that the total strain rate tensor $\dot{\boldsymbol{\varepsilon}}_{tot}$ can be separated into the creep, plastic and elastic strain rate tensors according to

$$\dot{\boldsymbol{\varepsilon}}_{tot} = \dot{\boldsymbol{\varepsilon}}_{cr} + \dot{\boldsymbol{\varepsilon}}_{pl} + \dot{\boldsymbol{\varepsilon}}_{el}. \tag{1}$$

During creep, the elastic strain $\boldsymbol{\varepsilon}_{el}$ decreases in favor of the creep strain $\boldsymbol{\varepsilon}_{cr}$, thus reducing the total stress $\boldsymbol{\sigma} = \mathbf{C} : \boldsymbol{\varepsilon}_{el}$ with $\mathbf{C}$ the elasticity tensor. It is sufficient to formulate the uniaxial creep law $\dot{\varepsilon}_{cr}(\sigma)$, where ε_{cr} and σ denote the equivalent strain and stress (von Mises stress), respectively. The full creep rate tensor, $\dot{\boldsymbol{\varepsilon}}_{cr}$, is then derived by choosing the creep strain updates normal to the yield surface (see [30]). The choice of the uniaxial creep law therefore determines the physics of the problem. In line with Goedecke and Mock [18], a Garofalo [31] or hyperbolic sine power creep law

$$\dot{\varepsilon}_{cr} = C_1 \sinh(C_2\sigma)^n \tag{2}$$

was adopted, which for small stresses σ, reduces to a power law as used by Brot et al. [6], and for high stresses to an exponential law as used by Brechet and Estrin [24], for example.

As the creep constant C_1 defines the characteristic time scale $\propto 1/C_1$ of the creep process, all results are presented using a scaled time

$$\tau = \frac{t}{t_1} = t\frac{EC_1}{H} \tag{3}$$

which was found in Goedecke and Mock [18] to render the results universal against changes in parameters E (Young's modulus), C_1 and H (hardness of the asperity). In the simulations, C_1 was therefore chosen to optimize numerical convergence. In reality, C_1 usually shows an exponential dependence on the temperature T; that is $C_1 = \tilde{C}_1 \exp(-Q_{cr}/kT)$ where Q_{cr} is the activation energy for creep. Moreover, C_1 varies widely even for small changes of material composition, let alone for material classes. At 400 K and for metals, values between 10^{-6} and $1\,s^{-1}$ are not out of the question, and reliable values are hard to achieve experimentally. In the further discussion, as an example, an iron-like material will be considered with an exemplary value of $C_1 = 10^{-3}\,s^{-1}$ (e.g., [32]).

For the main simulation loop, the testing of the creep model outlined in the following sections required a flexible application of boundary conditions and readout of simulation data from the finite element code. The default boundary condition was that of a constant force $F = F_{const}$, applied to the punch, as outlined in Fig. 1. The punch was therefore first quasistatically moved to the initial interference δ_{init} that corresponded to the reaction force F_{const}. The subsequent slow descent of the punch was then measured by reading the interference δ from the simulation, with the contact radius a being a secondary variable. The exponential nature of the creep law required a careful control of the integration time steps. A manual control of the integration times, with an exponential distribution of the time steps $t_i = t_{min} \exp(\theta i/N)$ with $\theta = \ln(t_{max}/t_{min})$ was used. Here, t_{min} and t_{max} denote the lower and upper limit of the simulation time frame and N the number of time steps, usually chosen as $N = 400$, depending on parameter choice.

Within this primary simulation loop, the simulation data was stored at every load step and, depending on the type of simulation conducted, a number of additional probing cycles could be inserted. The most simple probing cycle was a constant displacement ($\dot{\delta} = 0$) cycle. This is identical to the approach of Goedecke and Mock [18]. For this cycle, the force relaxation $\dot{F}$ was measured, allowing for a comparison with the results in [18]. The time steps were chosen to be extremely small, on the order of one hundredth of the corresponding time step used in the main (i.e., constant force) simulation loop. Therefore, an increase of the contact radius could usually not be detected between time steps and, for lack of better data, the radius a was assumed as constant.

For a second probing cycle, the simulation was reset to the stored configuration and in a quasistatic simulation ($t = const$), the change in punch reaction force (ΔF) was measured due to small changes in interference ($\Delta\delta$). For this experiment, a small change